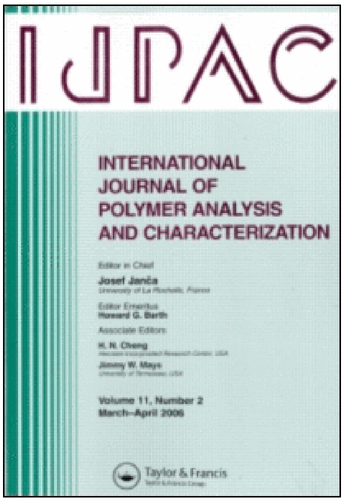

International Journal of Polymer Analysis and Characterization
Publication details, including instructions for authors and subscription information:
http://www.informaworld.com/smpp/title~content=t713646643

Fluorescence as a Characterization Tool to Study Amphiphilic Polymer Aggregation in Aqueous Media

Céline Frochot[ab]; Caroline Muller[a]; Alain Brembilla[bc]; Marie-Christiane Carré[a]; Pierre Lochon[b]; Marie-Laure Viriot[a]
[a] DCPR-GRAPP, UMR 7630 CNRS-INPL, Nancy [b] LCPM, UMR 7568 CNRS-INPL, Groupe ENSIC, Nancy [c] SRSMC-LCPOC, UMR 7565 CNRS-UHP, Faculté des Sciences, Nancy

To cite this Article Frochot, Céline , Muller, Caroline , Brembilla, Alain , Carré, Marie-Christiane , Lochon, Pierre and Viriot, Marie-Laure(2000) 'Fluorescence as a Characterization Tool to Study Amphiphilic Polymer Aggregation in Aqueous Media', International Journal of Polymer Analysis and Characterization, 6: 1, 109 — 122
To link to this Article: DOI: 10.1080/10236660008034653
URL: http://dx.doi.org/10.1080/10236660008034653

Int. J. Polym. Anal. Charact.,
2000 Vol. 6, pp. 109–122
Reprints available directly from the publisher
Photocopying permitted by license only

Fluorescence as a Characterization Tool to Study Amphiphilic Polymer Aggregation in Aqueous Media*

CÉLINE FROCHOT[a, b], CAROLINE MULLER[a],
ALAIN BREMBILLA[b, c], MARIE-CHRISTIANE CARRÉ[a],
PIERRE LOCHON[b] and MARIE-LAURE VIRIOT[a,†]

[a]*DCPR-GRAPP, UMR 7630 CNRS-INPL;* [b]*LCPM, UMR 7568 CNRS-INPL,*
Groupe ENSIC, 1, rue Grandville, F-54000 Nancy; [c]*SRSMC-LCPOC,*
UMR 7565 CNRS-UHP, Faculté des Sciences, F-54500 Vandœuvre les Nancy

(Received 31 October 1999; In final form 29 January 2000)

Fluorescence spectroscopy based on pyrene and DMAC (i.e., 1,1-dicyano-4-(4′-(*N,N*-dimethylamino)phenyl)-1,3-butadiene) probes was used to investigate the aggregation of amphiphilic polymers in aqueous solution. The fluorescence data related to the cohesion of the microdomains formed were correlated to the polymer microstructure, either by taking into account the sequence distribution for poly(NVP-*co*-C_{16}VIB) (i.e., poly(*N*-vinyl-2-pyrrolidinone)-*co*-(3-hexadecyl-1-vinylimidazolium bromide)) or the cryo-TEM images for poly(C_1VPB-*co*-C_{16}VPB) (i.e., poly(1-methyl-3-vinylpyridinium bromide)-*co*-(1-hexadecyl-3-vinylpyridinium bromide)).

Keywords: Fluorescence; Pyrene; DMAC; Polymers; Microstructure

INTRODUCTION

In recent years, a large number of studies dealed with the formation of hydrophobic microdomains in amphiphilic polymers and/or copolymers in water solution, especially with regard to their microstructure and the properties of the resulting molecular assemblies. Among these

---

[*] Presented at the 12th International Symposium on Polymer Analysis and Characterization (ISPAC-12), La Rochelle, France, June 28–30, 1999.

[†] Corresponding author. Fax: 33-3-83321099.

studies, the fluorescence spectroscopy was used as an optical method well suited to give the information about the change of the macromolecule conformation in aqueous media.[1-5] Fluorescent tracers, such as pyrene and molecular rotors (like DMAC), are particularly promising because their photophysical characteristics are sensitive to the modifications of the microenvironment whenever aggregation appears due to the increase of polymer concentration.

The amphiphilic polymers have a tendency to self-aggregate in an aqueous medium, due to the intra and/or intermolecular interactions of the long alkyl chains. Their physico-chemical properties are strongly dependent on the chemical nature of both the hydrophilic and hydrophobic moieties (respectively: cationic, anionic, non-ionic, etc. aliphatic, cyclic, aromatic, etc.) and, most importantly, their relative ordering in the macromolecular chain.[6] In order to establish a relationship between the molecular structure and the behavior of polymers in aqueous solution, random copolymers poly(NVP-*co*-C_{16}VIB) (Fig. 1) from 3-hexadecyl-1-vinylimidazolium bromide (C_{16}VIB, cationic part) with the spacing hydrophilic monomer *N*-vinyl-2-pyrrolidinone (NVP, nonionic part) were synthesized with various monomer feed compositions at low conversion rate, and their aggregation tendency studied using fluorescence spectroscopy. The polarity of the hydrophobic domains formed was sensed by both pyrene and molecular tracer DMAC. Moreover, the local microenvironment viscosity obtained from the fluorescence efficiency of the tracer DMAC was correlated to the molecular structure of the copolymers and their capacity for coiling.

In order to emphasize the potentialities of the fluorescence approach, we will recall previous results related to a series of copolymers,

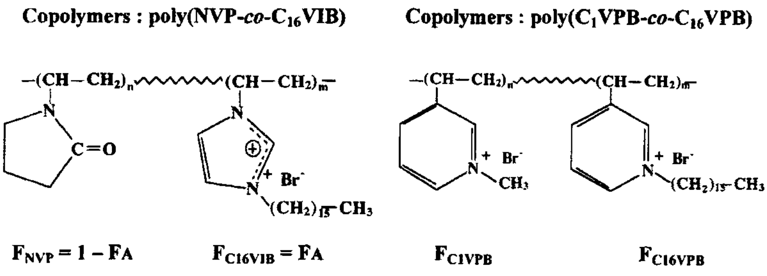

FIGURE 1 Molecular structures of copolymers described in this study.

poly(C_1VPB-*co*-C_{16}VPB) (Fig. 1), for which a correlation was also possible between fluorescence data and microstructure coming from cryo-TEM analysis.[7]

EXPERIMENTAL

Materials

The synthesis of the monomer 3-hexadecyl-1-vinylimidazolium bromide (C_{16}VIB) was described in a previous paper.[8] *N*-vinyl-2-pyrrolidinone (NVP) purchased from Aldrich was purified by distillation on a condensing cold surface.

The copolymers were prepared by mixing various molar fractions of C_{16}VIB and NVP (total amount of monomers $= 4 \times 10^{-2}$ mol) with 30 mL of ethanol, introduced in a reactor (50 mL), and degassed under vacuum by application of the freeze–thaw technique. Then 4×10^{-4} mol AIBN (Fluka, recrystallized from methanol) was added under Ar and the waterproof reactor was immersed, under stirring, in a thermostated bath at 60°C for times ranging from 5 to 20 min, according to the feed composition. The copolymerizations were stopped by cooling with liquid air. The copolymers were precipitated by the addition of acetone, filtered off, and then purified by a double dissolution in chloroform, followed by a precipitation by acetone. After drying under vacuum at 50°C for 24 hrs, the conversion ratios ($< 10\%$) were determined by weighing.

Methods

UV-visible Absorption and Fluorescence

Stock solutions were prepared by dissolution of the polymer in an aqueous mixture (1-propanol/water, 3/97, v/v). The absorption spectra were recorded on a Perkin Elmer (Lambda 2) (Germany) UV-visible spectrophotometer.

Fluorescence emission spectra were recorded on a SPEX Fluorolog-2 spectrometer equipped with a thermostatically controlled cell at 30°C.

For pyrene (1.1×10^{-6} M in the final solution), no excimer was observed; the samples were excited at 332 nm and the emission spectra of pyrene showed the vibronic peaks at $\lambda_1 = 372\,\text{nm}$ (I_1) and $\lambda_3 = 383\,\text{nm}$ (I_3) with a slit width = 0.5 mm ($\Delta\lambda_{1/2} = 1.88\,\text{nm}$).

For the tracer DMAC (3.3×10^{-6} M in the final solution), the spectra were recorded in the 500–600 nm range (slit width = 1.5 mm; $\Delta\lambda_{1/2} = 5.64\,\text{nm}$) and the excitation wavelength ($\lambda_{ex} = 511\,\text{nm}$) which generates only one single fluorescence peak.[9]

Copolymers Characterization

Copolymers compositions were determined by ^{13}C NMR using $CDCl_3$ as solvent. ^{13}C spectra were recorded on a Bruker AC-200 P (Germany) spectrometer.

RESULTS

Composition of the Copolymers Poly(NVP-*co*-C_{16}VIB)

The ^{13}C NMR spectra of the copolymers exhibit a peak at 176 ppm, which is characteristic of the carbon atom of the NVP carbonyl group. The resonance peak area (noted $S_{C=O}$) was compared with the total resonance area of all peaks (S_t) corresponding to the aliphatic carbon atoms of two units.[12] The FA and $1-FA$ denote the C_{16}VIB and NVP molar fractions respectively, FA is calculated from $S_{C=O}$ and S_t values according to the following equation:

$$\frac{S_t}{S_{C=O}} = \frac{5(1-FA) + 18FA}{1-FA} \tag{1}$$

The results are in good agreement with the data coming from the elemental analysis (based on the elemental analysis of Br present in the C_{16}VIB unit).

Fluorescence Studies of the Copolymers Poly(NVP-*co*-C_{16}VIB)

Pyrene as a Polarity Tracer

The pyrene represents a well known polarity probe, because of the vibronic structure dependence of its fluorescence with the polarity of the medium expressed as the ratio I_1/I_3, where I_1 and I_3 are, respectively, the emission bands 1 and 3 of the monomer spectrum.[10] Figure 2 shows the variations of the I_1/I_3 ratio for pyrene with concentration *c* of the different polymers (log scale). The decrease of I_1/I_3 extends over a relatively large range of concentrations. Except for the homopolymer poly(*N*-vinyl-2-pyrrolidinone) ($FA = 0$), the I_1/I_3 decreases from its highest value (around 1.89 with our apparatus, value in the mixture 1-propanol/water, 3/97, v/v) as the copolymer concentration increases, to reach a final plateau value. This value, characterizing the polarity in the surroundings of the tracer (hydrophobic microdomains), depends on the copolymer composition. As expected, the hydrophobic character of the tracer microenvironment increases as *FA* increases, *FA* being equal to the imidazolium units (or long chains C_{16}VIB) ratio in the copolymer. The lowest value for the I_1/I_3 was observed for the homopolymer containing long chain imidazolium moieties only ($FA = 1$).

From each curve, it is possible to determine the concentration c_m, which corresponds to the onset of the hydrophobic microdomains detected by the pyrene probe. c_m values range from 4.7×10^{-5} M for the most hydrophilic copolymer, i.e., $FA = 0.31$ to 1.7×10^{-5} M for

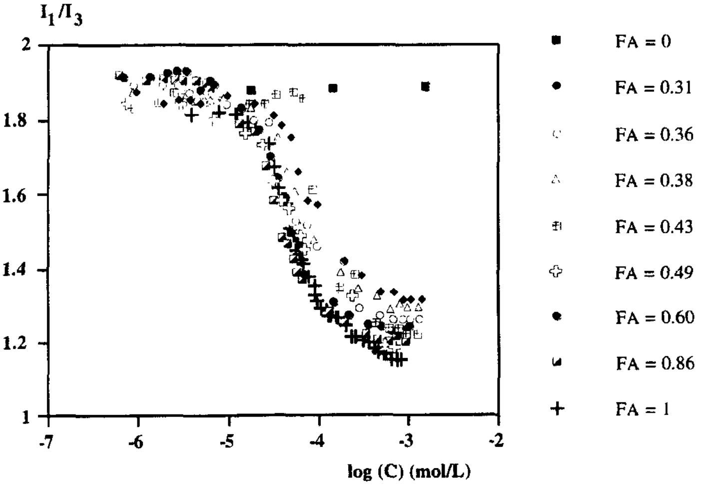

FIGURE 2 Variation of the ratio I_1/I_3 for pyrene versus polymer concentration. *FA* denotes FC_{16}VIB.

the homopolymer poly(C_{16}VIB), i.e., $FA = 1$. These values were determined by the graphic method, in which the value at the intersection of the upper horizontal line and the decreasing slope is taken.

It was also interesting to determine the pyrene binding constant K with the microdomains in relation to the hydrophobicity of the copolymers. The determination of the K value gives also a first indication on the capacity of the microdomains to incorporate the hydrophobic compounds for further solubilisation and transportation.

The distribution of pyrene between the bulk phase b and the microdomains phase m can be described by the following equation:[11]

$$K = \frac{[\mathrm{Py}]_m}{[\mathrm{Py}]_b(c - c_m)} \tag{2}$$

where $[\mathrm{Py}]_m$ and $[\mathrm{Py}]_b$ are the concentrations of pyrene in the microdomains and the bulk phase, respectively, c is the copolymer concentration and c_m is the concentration for which the microdomains are formed. By taking into account the separating phase model, the modeling of the curve I_1/I_3 vs. c allows the determination of both the association constant K and c_m. As expected from the calculations, the binding constant K increases with the long chain C_{16}VIB content in the copolymers (Fig. 3). The representative points for the K values

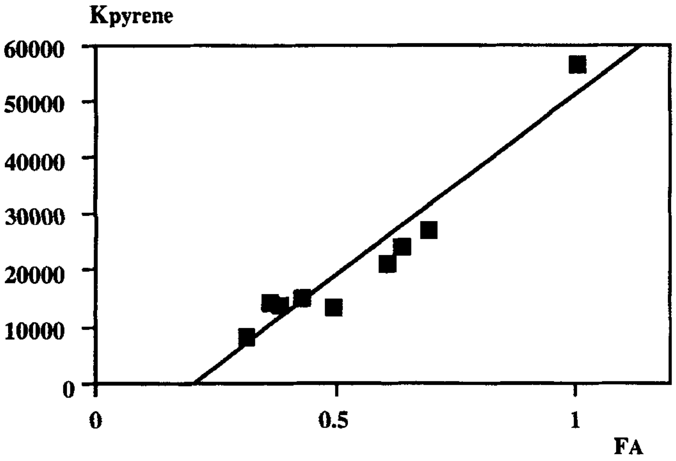

FIGURE 3 Variation of the binding constant K for pyrene versus C_{16}VIB molar fraction FA.

versus *FA* are distributed on a straight line: $K = 64000\ FA$ with a good linear relationship ($r^2 = 0.93$).

Fluorescent DMAC as a Polarity Tracer

We have previously shown that for the tracer DMAC, the fluorescence emission wavelength at its maximum is shifted to long wavelengths (bathochromic effect) when the polarity of the microenvironment is increased. This is similar to a decrease of $\bar{\nu}_{f\max}$ with an increase of polarity, as $\bar{\nu} = 1/\lambda$. The DMAC was largely used as a fluorescent probe to test the aggregation of the amphiphilic polymers.[5, 7, 9]

The Figure 4 shows the variations of $\bar{\nu}_{f\max}$ with the concentration *c* for different polymers (on a log scale).

The measured emission band wavelength $\lambda_{f\max}$ of DMAC shifted hypsochromically as the copolymer concentration increases. As shown in Figure 4, the $\bar{\nu}_{f\max}$ increases from around 16970 cm^{-1} (value in the mixture 1-propanol/water, 3/97, v/v) to a final plateau, the value of which depends on the C_{16}VIB units ratio (given by *FA*). As expected, the $\bar{\nu}_{f\max}$ (plateau value) increases as *FA* increases and the

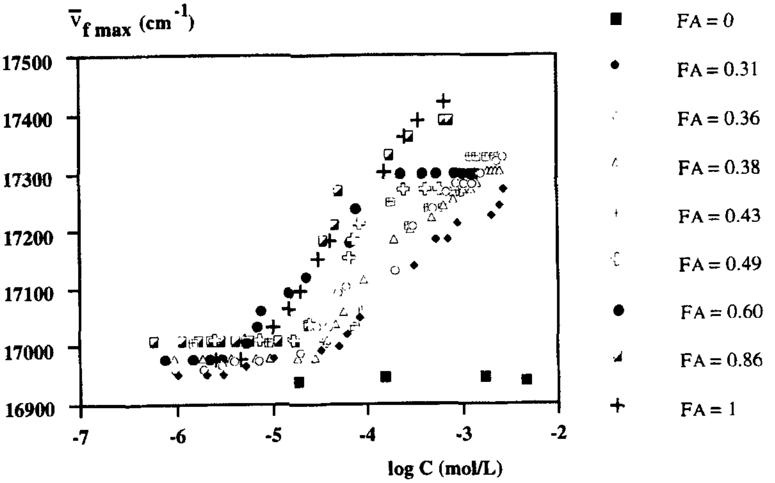

FIGURE 4 Variation of the fluorescent wavenumber $\bar{\nu}_{f\max}$ for DMAC versus polymer concentration.

largest deviation was observed for the homopolymer poly(C_{16}VIB) ($FA = 1$). In contrast, no variation was observed for the poly(NVP) ($FA = 0$).

Fluorescent DMAC as a Viscosity Tracer

We have shown previously that for the tracer DMAC, the fluorescence emission efficiency is sensitive to the local viscosity of the microenvironment, which plays a role on the nonradiative processes due, for a part, to the intramolecular rotational deactivation. Consequently, this fluorescent probe can also be an indicator of the cohesion of the structure. This property was particularly useful to study the aggregation of the amphiphilic polymers.[5, 7, 9]

The Figure 5 shows the variation of the Φ_f/Φ_{fo} ratio as a function of the polymer concentration (on a log scale) (where Φ_{fo} is the fluorescence quantum yield without the polymer in the medium). The quantum yield increases with concentration for all of the copolymers and the homopolymer poly(C_{16}VIB) ($FA = 1$) to reach a final plateau value. As expected, no variation occurs for the poly(NVP) ($FA = 0$).

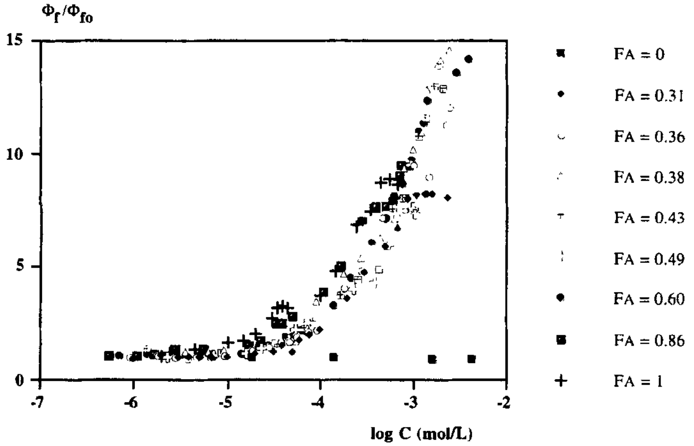

FIGURE 5 Fluorescence quantum yield Φ_f/Φ_{fo} ratio for DMAC versus polymer concentration.

DISCUSSION

Local Cohesion and Molecular Structure for the Copolymers Poly(NVP-*co*-C_{16}VIB)

For the copolymers, the probabilities P_{sequence} to find particular monomer sequences at low conversion ratio (< 10%) yield information on the ordering of C_{16}VIB and NVP moieties in the principal chain. A better image of the sequence distribution is given by the number-average lengths of C_{16}VIB and NVP runs, respectively:[12]

$$l_{C_{16}\text{VIB}} = 1 + r_{C_{16}\text{VIB}}z \quad \text{and} \quad l_{\text{NVP}} = 1 + (r_{C_{16}\text{VIB}}/z) \tag{3}$$

$$\text{with } r_{C_{16}\text{VIB}} = 0.5 \quad \text{and} \quad z = \frac{f_{C_{16}\text{VIB}}}{1 - f_{C_{16}\text{VIB}}} \tag{4}$$

where $f_{C_{16}\text{VIB}}$ is the molar fraction in the feed charge.

From the value of the ratio $l_{C_{16}\text{VIB}}/l_{\text{NVP}}$, we can propose a schematic representation of the principal chain for different copolymers (Tab. I). Then, taking this hypothetic molecular organization,

TABLE I Schematic representation of the principal chain for poly(NVP-*co*-C_{16}VIB) depending on *FA* values

FA (*FC*$_{16}$*VIB*)	$\bar{L}$ 16.*FA*[a]	$l_{C_{16}VIB}/l_{NVP}$	*Hydrophilic/ Hydrophobic balance*	*Expected organization in aqueous medium*
0.31	4.96	0.20		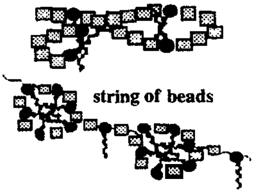
0.36	5.76	0.46	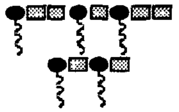	
0.38	6.08	0.47		
0.43	6.88	0.85		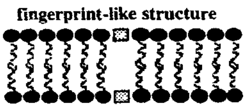
0.49	7.84	1.02		
0.60	9.60	1.50		
0.86	13.76	6.70		

[a] $\bar{L}$ represents a hydrophobic parameter.

we might correlate the fluorescence data of the tracer DMAC which reflects the cohesion of the hydrophobic microdomains formed, that means the plateau values of Φ_f/Φ_{f_0} for the tracer DMAC with the ratio $l_{C_{16}VIB}/l_{NVP}$ (Fig. 6).

At low C_{16}VIB content ($FA = 0.31$), the most plausible structure for the corresponding copolymer exhibits average sequences containing 5 NVP units per one C_{16}VIB unit, leading to a relatively unfolded macromolecular chain. For this copolymer, the local cohesion at the surroundings of the tracer, defined by Φ_f/Φ_{f_0}, indicates that it will not adopt a very organized structure in an aqueous medium (Fig. 6).

In contrast, when FA increases, for example for $FA = 0.49$, the $l_{C_{16}Vim}/l_{NVP}$ ratio becomes close to 1 and diads C_{16}Vim-NVP sequences are clearly predominant. This result is in agreement with the alternation tendency predicted from the low reactivity ratios. The fluorescence data are in agreement with a higher microdomains cohesion (maximal zone for the variation reported on Fig. 6). If we take into account the results coming from a recent study,[7] which was devoted to a comparison between fluorescence data and cryo-TEM images for a similar series of copolymers (see next section), we can put forward the assumption that the aggregation corresponds to an arrangement of the microdomains like a string of beads.

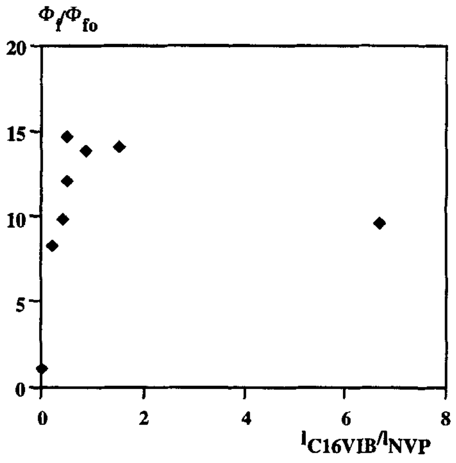

FIGURE 6 Variation of Φ_f/Φ_{f_0} (plateau values) for the tracer DMAC versus the ratio $l_{C_{16}VIB}/l_{NVP}$.

When the sequence of C_{16}Vim moieties increases further ($FA = 0.86$ and $l_{C_{16}Vim}/l_{NVP} = 6.7$), the ratio Φ_f/Φ_{f_0} decreases, indicating a lower compacity for the hydrophobic microdomains, in agreement with previous observations.[7] Indeed, a high content of long-linked alkyl chains seems to be unfavorable for compact arrangement of the microdomains. The aggregation rather leads to a bilayer-like structure, as the one previously found in cryo-TEM images for the similar series of copolymers (see next section).

Correlation Between Fluorescence Data and Microstructure for Two Series of Copolymers: Poly(NVP-*co*-C_{16}VIB) and Poly(C_1VPB-*co*-C_{16}VPB)

The influence of the copolymer composition (hydrophilic/hydrophobic balance) on the structure of the aggregates, was studied throughout the variations of the fluorescence characteristics of the tracer DMAC (plateau values) as a function of the parameter $\bar{L}$ which describes the relative contribution of the alkyl side chains to the copolymer structure.

The parameter $\bar{L}$ is defined by $\bar{L} = (ax + by)/100$, where x and y are the molar percent contents of each monomer in the polymer and a and b denote the carbon atom number of the alkyl side chains.[13]

For the copolymers poly(NVP-*co*-C_{16}VIB): $a = 0$ and $b = 16$, while x and y are the molar percent contents of NVP (i.e., $1 - FA$) and C_{16}VIB (i.e., FA) respectively, then $\bar{L} = 16y/100$ corresponds to the average length alkyl side chains per vinylimidazolium unit. For the copolymers poly(C_1VPB-*co*-C_{16}VPB): $a = 1$ and $b = 16$, while x and y are the molar percent contents of C_1VPB and C_{16}VPB respectively, then $\bar{L} = (x + 16y)/100$ corresponds to the average length alkyl side chains per pyridine unit.

Figures 7 and 8 represent variations of the fluorescence data for the tracer DMAC (plateau values for both emission wavelength and efficiency) as a function of the hydrophobicity parameter $\bar{L}$ for the copolymers poly(NVP-*co*-C_{16}VIB) and poly(C_1VPB-*co*-C_{16}VPB) respectively. For each series of copolymers, the compactness of the aggregates characterized by the value of the quantum yield ratio goes through a maximum for a given value of the hydrophobic parameter $\bar{L}$. For the poly(NVP-*co*-C_{16}VIB), this maximum corresponds

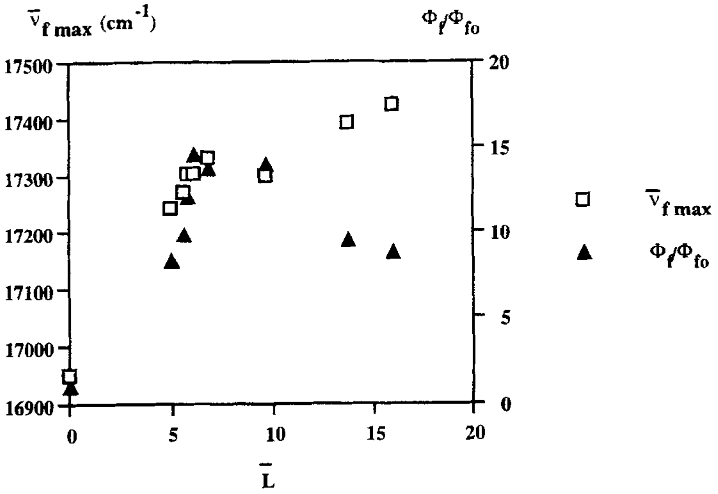

FIGURE 7 Variations of $\bar{\nu}_{f\max}$ and Φ_f/Φ_{fo} (plateau values) for the tracer DMAC versus the parameter $\bar{L}$ for the poly(NVP-*co*-C$_{16}$VIB).

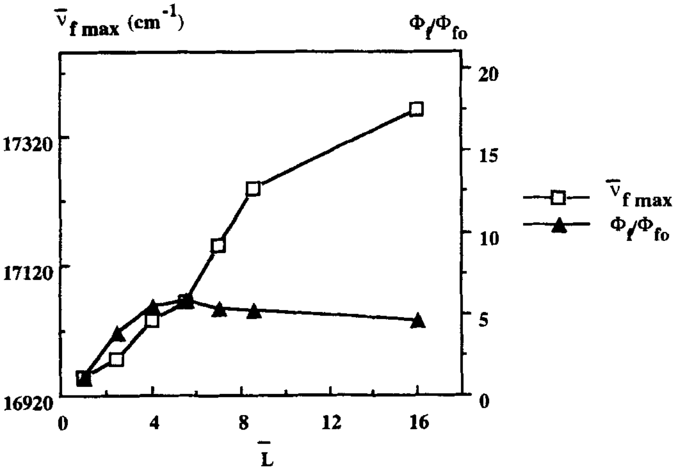

FIGURE 8 Variations of $\bar{\nu}_{f\max}$ and Φ_f/Φ_{fo} (plateau values) for the tracer DMAC versus the parameter $\bar{L}$ for the poly(C$_1$VPB-*co*-C$_{16}$VPB).

to, roughly, a *FA* value of 0.5, which means a string of beads-like structures (see Tab. I). For poly(C$_1$VPB-*co*-C$_{16}$VPB), this maximum corresponds to the copolymer containing 30% of hydrophobic units.

According to the cryo-TEM image,[7] this copolymer leads to a string-of-bead structure with small circles (diameter of the order of 5 nm) corresponding to the hydrophobic microdomains, which are connected by small segments.

Over the respective composition for the maximum fluorescence efficiency, the cohesion is rather lower (decrease of the ratio Φ_f/Φ_{fo}). This corresponds to a higher value of the parameter $\bar{L}$, which leads rather to the bilayer-like structures. Indeed, for the copolymers poly(C_1VPB-*co*-C_{16}VPB) with an hydrophobic part higher than 30% and for the homopolymer poly(C_{16}VPB), the cryo-TEM images clearly show dense objects, characterized by a spherical shape and a variable size, going from 20 to 70 nm, with a periodical structure of 3.4 nm, which illustrate the macromolecular chains regularly spaced out.[7]

Fluorescent Tracers as Polarity Sensors

For the copolymers poly(NVP-*co*-C_{16}VIB), two studies using respectively pyrene and tracer DMAC indicate identical behavior, i.e., lower polar character sensed by the fluorescent tracer, as the content of long-hydrophobic chain increases (see Figs. 2 and 4). A similar result was previously obtained for the poly(C_1VPB-*co*-C_{16}VPB).[9]

For each series of copolymers, an increase of the hydrophobic parameter $\bar{L}$ induces a constant decrease of the polarity character sensed by the tracer DMAC embedded in the aggregate (see Figs. 7 and 8 for the variations of $\bar{\nu}_{f\max}$).

CONCLUSION

This work shows the potential of fluorescent tracers to characterize the hydrophobic microdomains in aqueous medium for amphiphilic copolymers in relation to their chemical structure. The information covers the polarity aspect and also the local viscosity of the tracer microenvironment characterizing the cohesion of the copolymer.

In particular, the information linked to the local microenvironment viscosity of the tracer DMAC and obtained from its fluorescence quantum yield, is correlated to the molecular structure of the copolymers and their capacity of coiling: (i) in the case of copolymers of 3-hexadecyl-vinylimidazolium bromide/*N*-vinyl-2-pyrrolidinone, a relationship was established between the fluorescence quantum yield values and the molecular structure defined by the number average length of the sequence distribution of the monomers, and, (ii) in the case of poly(1-methyl-3-vinylpyridinium-*co*-1-hexadecyl-3-vinylpyridinium dibromide), a parallel was drawn between the fluorescence quantum yield values and the organization modes of the macromolecular chains observed by cryo-TEM.

References

[1] F. M. Winnik (1993). *Chem. Rev.*, **93**, 587.

[2] W. Binana-Limbelé and R. Zana (1990). *Macromolecules*, **23**, 2731.

[3] A. Fischer, M. C. Houzelle, P. Hubert, M. A. V. Axelos, C. Geoffroy, M. C. Carré, M. L. Viriot and E. Dellacherie (1998). *Langmuir*, **14**, 4482.

[4] S. Tazuke, R. K. Guo, T. Ikeda and T. Ikeda (1990). *Macromolecules*, **23**, 1208.

[5] A. Benjelloun, A. Brembilla, P. Lochon, M. Adibnejad, M. L. Viriot and M. C. Carré (1996). *Polymer*, **37**, 879.

[6] P. Anton, P. Köberle and A. Laschewsky (1993). *Makromol. Chem.*, **194**, 1.

[7] A. Benjelloun, C. Dorion, A. Brembilla, M. L. Viriot and M. Adrian (1998). *Macromol. Symp.*, **127**, 165.

[8] A. Benjelloun, C. Damas, A. Brembilla and P. Lochon (1994). *Polym. Bull.*, **33**, 513.

[9] C. Damas, M. Adibnejad, A. Benjelloun, A. Brembilla, M. C. Carré, M. L. Viriot and P. Lochon (1997). *Colloid Polym. Sci.*, **275**, 364.

[10] D. C. Dong and M. A. Winnik (1984). *Can. J. Chem.*, **62**, 2560.

[11] M. Wilhelm, C. L. Zhao, Y. Wang, R. Xu, M. A. Winnik, J. L. Mura, G. Riess and M. D. Croucher (1991). *Macromolecules*, **24**, 1033.

[12] C. Damas, S. Baggio, A. Brembilla and P. Lochon (1997). *Eur. Polym. J.*, **33**, 1219.

[13] S. Shinkai, S. I. Hirakawa, M. Shimomura and T. Kunitake (1981). *J. Org. Chem.*, **46**, 868.